

1 **Macroscopic Traffic Dynamics in Urban Networks**
2 **during Incidents**

3
4
5
6 **Sasan Amini (Corresponding Author)**

7 Chair of Traffic Engineering and Control

8 Technical University of Munich, Arcisstr. 21, 80333 Munich, Germany

9 ORCID: 0000-0002-1675-4945

10 Email: sasan.amini@tum.de

11
12 **Gabriel Tilg**

13 Chair of Traffic Engineering and Control

14 Technical University of Munich, Arcisstr. 21, 80333 Munich, Germany

15 ORCID: 0000-0001-9167-0680

16 Email: gabriel.tilg@tum.de

17
18 **Fritz Busch**

19 Chair of Traffic Engineering and Control

20 Technical University of Munich, Arcisstr. 21, 80333 Munich, Germany

21 ORCID: 0000-0002-2194-548X

22 Email: fritz.busch@tum.de

23
24
25 Word count: 5325 words + 2 table(s) \times 250 = 5825 words

26
27
28 Submitted January 13, 2020

29
30
31
32 Paper submitted for presentation at the 99th Annual Meeting Transportation Research Board,
33 Washington D.C., January 2020

1 **ABSTRACT**

2 The degradation of road network performance due to incidents is a major concern to traffic oper-
3 ators. The development of urban traffic incident management systems requires a comprehensive
4 understanding of traffic dynamics during incidents. Recently, the concept of the macroscopic fun-
5 damental diagram (MFD) contributed to such an understanding and has been used in a wide range
6 of applications. However, the MFD is merely reproducible under recurring traffic patterns. Mo-
7 tivated by a few studies which argue the existence of the MFD with a clockwise hysteresis loop
8 during incidents, we tackle this limitation of the MFD and propose a framework to study the char-
9 acteristics of the MFD under non-recurring congestion. More specifically, we introduce a criticality
10 score (CS) which represents network redundancy and postulate that links with a higher level of CS
11 impose a larger hysteresis loop on the MFD. We design an experiment in a microscopic traffic
12 simulation to study the relation of closed links and the resulting MFDs. The results confirm our
13 postulation and we observe that links with similar CS have a comparable impact on the shape of
14 the MFD. The main contribution of this paper is the possibility to develop a framework for inci-
15 dent detection in urban networks under limited sensor coverage. However, the findings of the study
16 may strongly rely on the assumptions, for instance, the network structure, the OD pairs, and drivers
17 route choice during incidents. Thus, future studies are required to study other network topologies
18 as well as more realistic driver route choice during incidents.

19 *Keywords:* Incident detection, Urban traffic, Macroscopic Fundamental Diagram, Hysteresis loops

1 INTRODUCTION

2 With the growth of traffic volumes in urban networks, traffic congestion has become a major concern for both citizens and city authorities. It increases travel time, air pollution and reduces economic productivity, safety, and quality of life. Generally, there are two types of congestion: (i) recurring congestion that occurs regularly when demand exceeds the road capacity, for example, every day during peak hours, and (ii) non-recurring congestion which is caused by incidents or planned special events which either temporarily reduce supply or suddenly increase demand. It is critical to distinguish these two as their required countermeasures are inherently different. The degradation of road network performance due to non-recurring congestion, hereafter called incidents, is a much bigger concern to traffic operators.

11 Incidents are generally defined as situations where the observed traffic state significantly deviates from its prediction (1). Most of the incident detection methods base their algorithm on this logic and hence, all of them, in some form or another, are comparative algorithms (2). Incident detection methods can be divided into two very broad groups. First, parametric statistical methods such as the class of time series analysis or state-space models, as well as non-parametric models which include the family of machine learning techniques e.g. neural networks or support vector machines. Second, methods that are based on the traffic flow theory such as e.g. McMaster Algorithm (3).

19 The latter group mainly consists of methods that are based on the well-known fundamental diagram of traffic flow. The advantage of these models in comparison to the previous group is that they use explanatory variables that characterize traffic dynamics. However, the notation of the fundamental diagram is limited to uninterrupted facilities. Consequently, these incident detection algorithms e.g. (4, 5) are mainly confined to freeway segments. Nonetheless, a limited number of studies have been conducted to develop similar incident detection in urban arterials. Bell and Thancanamootoo (6) were the first to use flow and occupancy data from loop detectors of adaptive traffic signal control system SCOOT to detect incidents. Sethi et al. (7) have developed two distinct algorithms for fixed loop detectors and probe vehicles that can be applied on single links. However, these methods are extremely biased and depend on the positioning of the detectors, probe penetration rate, the time resolution of data and fail to detect the congestion where no detector is available e.g. if traffic diverges on the upstream links.

31 The group of incident detection methods mentioned first handles the problem of incident detection mostly as temporal outlier detection in single-profile sensor data using signal processing techniques. These methods have emerged from other fields such as wireless sensors or internet traffic analysis and vary from simple boxplot methods to support vector machines (8). However, these methods face two challenges. First, they often require labeled data as ground truth or rely on a priori data distributions. In reality, however, such information is rarely available for urban traffic. Data are often noisy and might be recorded by malfunctioning sensors. Second, urban road networks as a physical system have much more complicated dynamics in comparison to wireless sensor networks. Nevertheless, various researchers have applied these methods on urban networks to detect incidents.

41 For instance, Anbaruglu et al. (9) proposed a spatiotemporal clustering approach to detect non-recurring congestion in London using travel time data from automated number plate recognition (ANPR) cameras. They employ a global constant factor to decide whether the travel time of a link is exceeding the normal level. Such an assumption will not represent the heterogeneity of urban traffic dynamics. The authors extended their work in a follow-up (10) and relaxed the as-

1 sumption of a constant congestion factor by proposing a space-time scan statistics which annotates
2 congestion as non-recurring if the difference between current and historical travel times is statis-
3 tically significant. In another study, Zhang et al. (11) use dictionary-based compression theory to
4 identify the features of both spatial and temporal patterns by analyzing multi-dimensional traffic-
5 related data. We briefly review some of these studies in Section 2 to present a comprehensive
6 oversight.

7 Both of these two groups of methods require large historical data sets and extensive sensor
8 networks, which are not available in many cities. Moreover, they are mainly applied for incident
9 detection. They do not evaluate the network performance, and thus, cannot be used to develop
10 proper traffic management strategies. In this paper we try to fill this gap by characterizing the
11 impact of incidents on the performance of urban networks using recent findings in traffic flow
12 theory i.e. the concept of the macroscopic fundamental diagram (MFD). Recently, several studies
13 suggesting that instability in network caused by major disturbances imposes clockwise hysteresis
14 loops in the MFD were published. The question is if the disturbances based on their impact on
15 the shape of MFD can be clustered and use such clusters to detect similar exogenous instabilities.
16 The contribution of the paper is twofold. First, we propose a framework that can not only be
17 used for incident detection but also for development of efficient traffic management strategies to
18 alleviate incidents impacts. Secondly, we study the properties and characteristics of MFD during
19 non-stationary states which has received very little attention.

20 The remainder of this paper is structured as follows. The theoretical background and prop-
21 erties of the MFD is provided in Section 2. Then we introduce our approach for characterization
22 of incidents in urban networks in Section 3. In Section 4 we present a microscopic traffic simu-
23 lation case study to evaluate the efficiency of the methodology. The results of this case study are
24 discussed in Section 5. We provide conclusions and directions for future work in Section 6.

25 THEORETICAL BACKGROUND

26 Macroscopic Fundamental Diagram

27 The original idea of a macroscopic relationship between network outflow and accumulation was
28 first introduced by Godfrey (12). Several researchers postulated a similar relationship (13, 14, 14)
29 and Mahmassani (15) tested it in a simulation experiment. But it was only after the work of Da-
30 ganzo and Geroliminis (16, 17) that the MFD gained attention. Inspired by their findings on data
31 from Yokohama, many other researchers have observed a similar relationship in empirical data
32 from several cities such as Toulouse, France (18), Brisbane, Australia (19), Zurich, Switzerland
33 (20), Lucerne, Switzerland, and London in the United Kingdom (21), as well as in traffic simu-
34 lations (22, 23, 24). The MFD is arguably network-specific and a function of network topology,
35 signal control settings and route choice (22, 23). This has made it a valuable tool to develop a
36 wide range of traffic control applications such as routing strategies (25, 26, 27), perimeter traffic
37 control (28, 29), on-street parking (30, 31) and congestion charging (21). While influential factors
38 on the shape of MFD has been well studied under steady states, empirically derived MFDs exhibit
39 multivaluedness and hysteresis loops which need to be further investigated.

40 Bifurcation and Hysteresis Loops in the MFD

41 Bifurcation or hysteresis loops are certain types of multivaluedness in the MFD where two groups
42 of flow values for a given range of density are observed.

43 The first empirical hysteresis loop was reported in Toulouse (18) where on a particular day

1 due to a social movement of truck drivers between 8 and 10 in the morning the speed on the city's
2 ring road drops and causes drivers to search for alternatives. Motivated by this observation, Gayah
3 and Daganzo (32) showed that even in a perfectly symmetric network with uniform demand, a
4 hysteresis loop forms during network unloading. They identify four types of MFD paths i.e. the
5 single-path, the clockwise loop, the counterclockwise loop, and the figure-Eight. They conjecture
6 that during recovery, when more trips are ending than starting, the network has a tendency towards
7 uneven congestion distribution which results in a clockwise hysteresis loop. Saberi et al. (33, 34)
8 have observed a similar phenomenon in a freeway network. Others have studied the potential rea-
9 sons for hysteresis-like patterns in the MFD (25, 35, 36). Sim et al. (36) propose four possible
10 reasons for bifurcation in empirical MFD: network heterogeneity, trip completion rate, detouring
11 pattern, and commuting trips. Geroliminis and Sun (37) have conducted a thorough analysis of net-
12 work heterogeneity and argue that hysteresis is a result of multiple congestion pockets of different
13 size which are not necessarily interconnected. Since arterial networks offer a higher degree of re-
14 dundancy, drivers adaptively change their routes to identify less congested links. Consequently, the
15 distribution of congestion is more homogeneous whereas freeway networks are not redundant and
16 therefore, congestion propagates unevenly. This assumption may not hold during non-recurring
17 congestion especially when drivers cannot make perfect route choices. For example, in an empiri-
18 cal study in Brisbane, Australia (19) an abnormal scatter and capacity drop is observed because of
19 an accident on a major arterial resulting in a road closure during morning peak hours. The authors
20 concluded that if network partitioning is performed, MFD can be used to detect incidents.

21 The literature in this particular line of research i.e. the shape of MFD during non-recurring
22 congestion is very limited. For instance, Zockaie et al. (38) study the shape of the MFD during the
23 evacuation of a large-scale city. They conclude that adaptive drivers increase fluctuations in the
24 MFD but reduce hysteresis and improve capacity. In a more recent study, Kim et al. (39) use the
25 concept of MFD to develop a novel link criticality index. They remove a link from a network and
26 assume the duration of the closure is short enough that neither a new user equilibrium is formed nor
27 OD demand changes significantly. The authors focus only on network loading and incrementally
28 increase a random demand function until the network reaches gridlock. The obtained MFD shows
29 slightly lower flow for the same density of the normal operation, lower capacity but the same value
30 near jam density. Based on this performance loss, the criticality of each link is evaluated. Lastly,
31 Horiguchi et al. (40) propose a mesh-wised network monitoring framework to detect anomalous
32 congestion. They introduce a fluidity indicator which is based on the distance of the obtained
33 MFD point from the origin (0,0) and a singularity indicator which shows the probability to observe
34 a point at a certain time of day. In consideration of these studies, the question arises if similar
35 disruptions in dense urban networks cause comparable deviations in the shape of the MFD.

36 **METHODOLOGY**

37 In this section, we propose the methodology for the analysis and characterization of traffic flow dy-
38 namics during incidents in urban networks. It is based on the concept of the MFD and is composed
39 of two main parts. The first part deals with the criticality of each link in a network by introduc-
40 ing a criticality score (CS) that reflects the impact of closing each road on the performance of the
41 network. The second part of the methodology quantifies the properties of MFDs using a set of
42 explanatory variables.

43 Then, for a given network with predefined OD demand, we postulate that closing links with
44 similar CS results in a comparable change in the shape MFD. In other words, the characteristics

1 of the scatter and hysteresis loop imposed on the flow-density plane of the MFD by an incident
 2 can be related to a set of features explaining how critical that link is for the network. Quantifying
 3 the impact of incidents and linking them to the characteristics of the network allows us to detect
 4 incidents under incomplete sensor coverage and improve network performance by implementing
 5 efficient traffic management measures. Please note that the main assumption is that demand is
 6 recurrent. This implies that any deviation from the expected MFD curve is caused by exogenous
 7 disruptions.

8 **Criticality Score**

9 First, we define our criticality score (CS), which is similar to the definition of betweenness central-
 10 ity in graph theory, generalized for directed graphs by White and Borgatti (41). In network science,
 11 edge Betweenness centrality is often applied to indicate how critical an edge is to a given graph. It
 12 is defined as the fraction of shortest paths between all pairs of nodes passing through an edge. A
 13 higher value of a betweenness centrality represents a bridge-like connector between two parts of a
 14 graph. The removal of such a connector may affect the shortest path between many pairs of nodes.
 15 In transportation networks, shortest paths are usually defined based on generalized cost including
 16 distance, travel time, comfort etc. which are time-varying and depend mostly on the level of con-
 17 gestion. Calculating such a dynamic cost function requires a comprehensive understanding of the
 18 network, which is usually missing. In addition to the length of the shortest path, it is important to
 19 evaluate the number of existing alternatives for the shortest path. This feature is usually referred
 20 to as redundancy and considers the number of alternative paths for a given OD pair. In the case
 21 of a road closure, redundancy plays a vital role in compensating the impacts of closure through an
 22 even distribution of congestion. Hence, it is a critical feature of the network. Therefore, instead
 23 of betweenness centrality, we propose a simpler alternative approach focusing only on redundancy
 24 for homogeneous networks i.e. networks with links with identical fundamental diagram, equal
 25 length and traffic signal configuration as follows.

26 Let $\mathcal{G}(V, E)$ be a directed graph representing the road network where V and E are the sets of
 27 nodes and edges, respectively. We denote the adjacency matrix of the network by \mathcal{A} and calculate
 28 the number of all shortest paths between each pair of nodes. Using simple graph theory, one can
 29 prove that the number of paths with length k between node i and j is the $(\mathcal{A}^k)_{ij}$ where \mathcal{A}^k is k th
 30 power of Matrix \mathcal{A} . In other words, the number of paths with length k from node i to node j is
 31 equal to the element $a_{i,j}^k$ of matrix \mathcal{A}^k . Thus, the total number of all possible paths for network \mathcal{A}
 32 from length of 1 to maximum possible length k_{max} is:

$$N_p^A = \sum_{(i,j)} \sum_{k=1}^{k_{max}} a_{ij}^k \text{ for } (i, j) \in V \times V \quad (1)$$

33 We define the CS of a link by the reduction in the total number of paths once we close that link
 34 $CS_l = N_p^A - N_p^{A^l}$. A^l represents the adjacency matrix of the network after removal of link l . Higher
 35 values of CS indicate that more drivers must be rerouted to reach their destination and some links
 36 become oversaturated due to lack of alternative routes between the first-order adjacency of the
 37 closed link. Such an assumption implies that drivers learn about the closure just before they reach
 38 the closed road which is realistic in case of unexpected incidents. In our use case, this is par-
 39 ticularly important because as suggested in the literature (33) adaptive drivers have a significant
 40 influence on the shape of hysteresis loops and network capacity. Please note that this is only true

1 for homogeneous networks with an existing MFD.

2 **Characterization of the MFD Hysteresis Loop**

3 In order to categorize the incidents, we must quantify their impacts on the MFD. We use a set of
 4 explanatory variables to measure the differences between two MFDs. Saberi and Mahmassani (34)
 5 have characterized the hysteresis loop by its shape. They describe a loop by its height Δq , width Δk ,
 6 and the area covered by this rectangular $S_H = \Delta q \times \Delta k$. However, these variables are not enough
 7 to identify a hysteresis loop uniquely. For example, as it is shown in Figure 1, two hysteresis loops
 8 can have an identical area but one (MFD 2 in Figure 1) shows higher average speed. Thus, we take
 9 into account the average speed of traffic states related to the hysteresis loop. Furthermore, incidents
 10 cause a capacity loss in the MFD which should be measured as well denoted by q_{ni} . Additionally,
 11 it is important to consider the number of observations that form the hysteresis loop, as an indicator
 12 for the duration of instability in the MFD. Table 1 summarizes the explanatory variables to describe
 13 the MFD. It is important to note that we avoid replacing density with occupancy to reduce potential
 14 error sources while converting occupancy to density. Only for the calculation of average speeds,
 15 we assume an average vehicle length of 5 m and a detector length of 2 m.

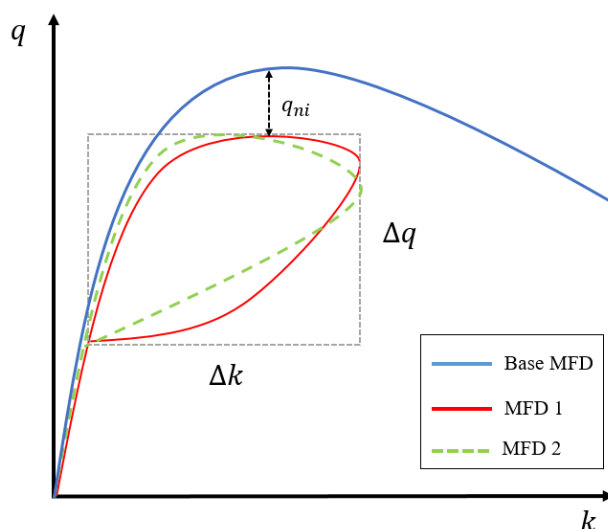


FIGURE 1 : Explanatory variable for hysteresis loops characteristics

TABLE 1 : Explanatory variables to describe MFD with hysteresis loop

Variable	Explanation	Unit
q_{ni}	capacity loss	(veh/h/ln)
Δq	flow drop (loop height)	(veh/h)
Δo	occupancy changes (loop width)	(%)
S_H	area of the loop approximated by rectangular	(veh/h)(%)
\bar{v}_H	average speed over the hysteresis loop	(km/h)

1 SIMULATION EXPERIMENT

2 In this section, we present the framework of a microscopic simulation experiment to investigate
3 our initial postulation and show the results. The discussion on the obtained results is provided
4 in section 5. For the simulation, we use the microscopic traffic simulation SUMO (42). Please
5 note that we are neither aiming at evaluating a realistic scenario nor questioning the equilibrium
6 condition during incidents. The primary goal is to study a controlled environment where drivers
7 route choice behavior remains manageable. Our toy network is represented by a unidirectional grid
8 of size 5×5 to reduce the problem size. Such a network can represent an urban network with strong
9 directional flows e.g. high demand during morning peak towards the city center. Grid networks
10 were previously used for investigating the relationship between route choice and the shape of the
11 MFD (24, 25, 43, 44). The network is composed of 60 nodes from which 12 (South and West
12 side) are only origins, 12 are only destinations (North and East side) and the 36 in the middle are
13 signalized intersections with 90 s of cycle length and 40 s of green time without any offset. The
14 network consists of 60 links with a length of 300 m, each with two lanes and a speed limit of
15 50 km/h. We put one loop detector on both lanes of each link. The data aggregation interval is
16 set to 3 minutes. The distance to the stop line is drawn from a uniform distribution for each loop
17 detector. This results in an MFD with little bias as suggested by (43). Additionally, we relax the
18 assumption of complete sensor coverage and investigate the MFDs based on randomly selected
19 30% of all detectors. Yet, we observe similar results for this case. We exclude measurements
20 at the generation and destination links as they may cause significant bias in our network variable
21 calculations.

22 The demand incrementally increases along with origin links as shown in Figure 2, where
23 q_{in} is additionally incrementally increased over time. The duration of the simulation is 2 hours
24 and 30 minutes, plus 15 minutes in the beginning for warm-up and 15 minutes in the end for
25 egress. For the first hour the demand is increased by a factor between 2 and 8 every 15 minutes
26 and similarly decreases during the second hour. To ensure congestion does not only appear at the
27 boundary edges where inflows are added, we add some random trips in the network with different
28 trip lengths during these two hours to ensure some traffic is cruising in the network as background
29 congestion. We purposefully replicate similar network configuration used in (44) to compare our
30 results with their findings. We compare the MFDs from several scenarios: a base scenario in
31 which we use the demand profile described above and seven different road closure scenarios in
32 each of which a different link is closed from the beginning to the end of the simulation. Drivers
33 are not informed about this incident and those who originally traverse the closed link to reach their
34 destination are only informed about the closure one intersection upstream of the closed road and
35 only then start to look for the fastest alternative. In case there is no alternative available, the closest
36 destination node is assigned to the vehicle as its new destination. This occurs only to vehicles that
37 must drive straight all the way.

38 Base Scenario

39 The base scenario represents a dynamic user equilibrium condition that is achieved by setting the
40 maximum relative standard deviation of travel time for each OD pair to 0.01 as the convergence
41 criterion. The MFD obtained from this scenario serves as our benchmark MFD to which we com-
42 pare the other MFDs from incident scenarios. Figure 3 shows a small clockwise hysteresis loop
43 during network unloading from 08:00 to 08:45. During this time the standard deviation of occu-
44 pancy across the links of the network reaches its maximum value. This is a common phenomenon

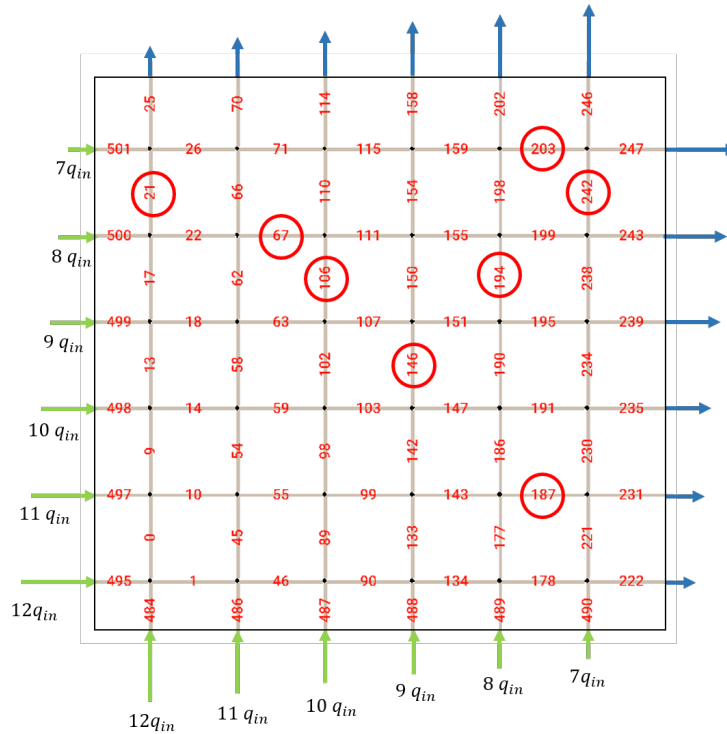


FIGURE 2 : The studied grid-network with the inflow and outflow at its boundaries. Edge IDs with a red circle around their ID are studied for closure scenarios

- 1 observed in many other simulation and empirical studies as discussed in Section 2. Please note
- 2 the smaller loop, right after the hysteresis loop ends, is caused by a sudden increase in network
- 3 accumulation at 08:45.

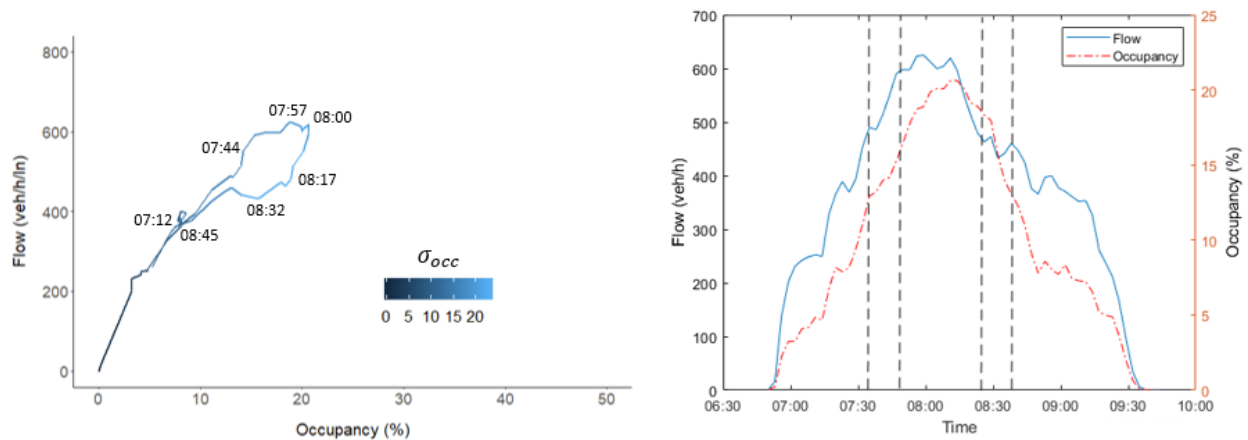


FIGURE 3 : Left: MFD from the base scenario. The standard deviation of occupancy is maximum during unloading part of the hysteresis loop. Right: time series of flow and occupancy showing lower flow for the same occupancy level during unloading.

1 Incident Scenarios

2 In total, we conduct 8 different incident scenarios by closing links 242, 203, 194, 187, 146, 106,
 3 67 and 21 which can be seen in Figure 2. In order to compare the scenarios, we first calculate the
 4 criticality of each link using the introduced CS in section 3. Together with the characteristics of the
 5 hysteresis loop obtained from the MFD of each scenario we present an overview of each scenario in
 6 Table 2. Generally, the capacity loss q_{in} decreases linearly as the value of CS decreases. However,
 7 there is an exception for the scenario where links 106 and 21 are closed. A possible explanation
 8 for this is the strong directional flow in the network from bottom left to the top right. The spillback
 9 caused by the closure of these links would extremely limit overall vehicular flow since they are
 10 closer to the entry point of demand. In an extreme case, closure of link 21 blocks almost all the
 11 possible inflow from the left side of the network resulting in a different demand scenario and thus
 12 is not further discussed. Due to the symmetrical topology, links 242 and 203 have identical CS
 13 values but due to randomly generated background traffic, the MFDs in these two scenarios are not
 14 identical. This can be clearly seen in the capacity drop and the size of the hysteresis loop.

15 For a better understanding, we compare the links with a similar CS and plot three groups
 16 of MFDs as it is shown in the top row of Figure 4. We can see that higher values of CS impose a
 17 larger hysteresis loop on the MFD. Moreover, we can easily observe the congested branch of MFD
 18 in scenarios 243 and 194. The spillback caused by the closure of these links propagates back to the
 19 origins and brings the network close to gridlock. The larger size of the loop implies longer queues
 20 and a spillback near to the closed link while other links of the network are in free-flow state. As
 21 mentioned above, these observations also hold for the case that only 30 % of all links are equipped
 22 with loop detectors.

23 Another important metric for the analysis of macroscopic traffic dynamics is the trip com-
 24 pletion rate which was originally used in (17). It is defined as the number of vehicles exiting the
 25 network to the number of vehicles in the network. The decrease in this rate indicates lower network
 26 production if the average trip length remains unchanged. The bottom row of Figure 4 depicts the
 27 trip completion rate for the three pairs of scenarios. Similar to their MFDs, we observe that the
 28 changes in trip completion rates are also very similar in scenarios with close CS values. Please
 29 note that this rate is not constant due to changes in average trip length in the network during the
 30 loading and unloading phase.

31 By carefully analyzing the MFDs and the trip completion rate time series, we can observe
 32 that in all the scenarios the point at which MFDs during incident situations deviate from the base

TABLE 2 : Criticality score and the characteristics of the hysteresis loop for each scenario

Closure scenario	Link CS	q_{ni}	Δq	Δo	S_H	\bar{v}_H
link-242	126	469	262	11.4	2986	31.8
link-203	126	413	206	11.1	2286	31.7
link-194	90	490	202	10.2	2424	34.7
link-146	60	501	122	6.14	749	37.8
link-106	40	440	121	4.94	597	38.0
link-67	20	542	147	3.93	577	38.2
link-187	5	566	118	3.37	397	38.6
link-21	1	445	315	6.63	2088	37.5

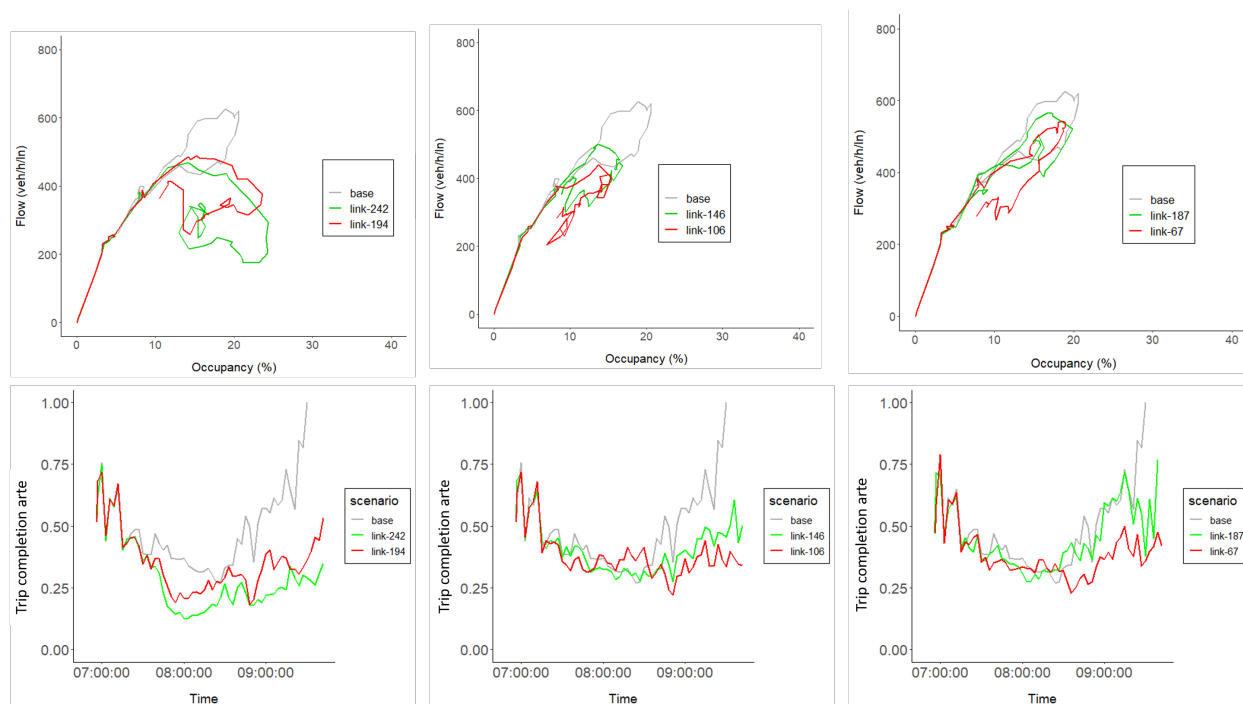


FIGURE 4 : Top: Similar scenarios exhibit comparable hysteresis loops in the MFD. Bottom: trip completion rate for the similar groups of scenarios follow comparable pattern.

1 scenario MFD is at occupancy of around 8% and flow of 400 veh/h/ln. Moreover, the time at which
 2 this splitting happens is more or less identical in all of the scenarios. We will discuss the reasons
 3 for this in the next section.

4 Network heterogeneity is a well-studied factor that affects the shape of MFD by inducing
 5 scatter and hysteresis loops. Thus, it is necessary to investigate the existence of heterogeneity in
 6 more detail. The most common measure to quantify it is the standard deviation of occupancy. The
 7 distribution of congestion across the network at different time intervals of the simulation is illus-
 8 trated in Figure 5. We can see that in some situations some links are fully congested (occupancy
 9 100 %) and some other empty (occupancy 0 %). This happens for scenarios in which a link in the
 10 middle of the grid network is closed than a link at closer to destination links. By comparing the
 11 first and the second row of the histograms, we observe that both mean and standard deviation of
 12 occupancy are increasing. Whereas in the third row of histograms, both values decrease again and
 13 reach values similar to the ones in the histograms in the first row. Overall, this analysis confirms
 14 the distribution of congestion in scenarios 187 and 67 is closer to the base scenario as indicated by
 15 the associated MFDs.

16 DISCUSSION

17 After presenting the result of our simulation experiment, we discuss the findings and limitations
 18 of our approach. We compare our results to studies that have used the concept of the MFD under
 19 other non-recurring congestion and seek potential generalization of the findings.

20 First of all, we can confirm our initial postulation and conclude that more critical links in
 21 the network induce larger hysteresis loop and higher capacity loss in the MFD. These results are
 22 in line with those from (39) who have earlier used the concept of the MFD to develop a criticality

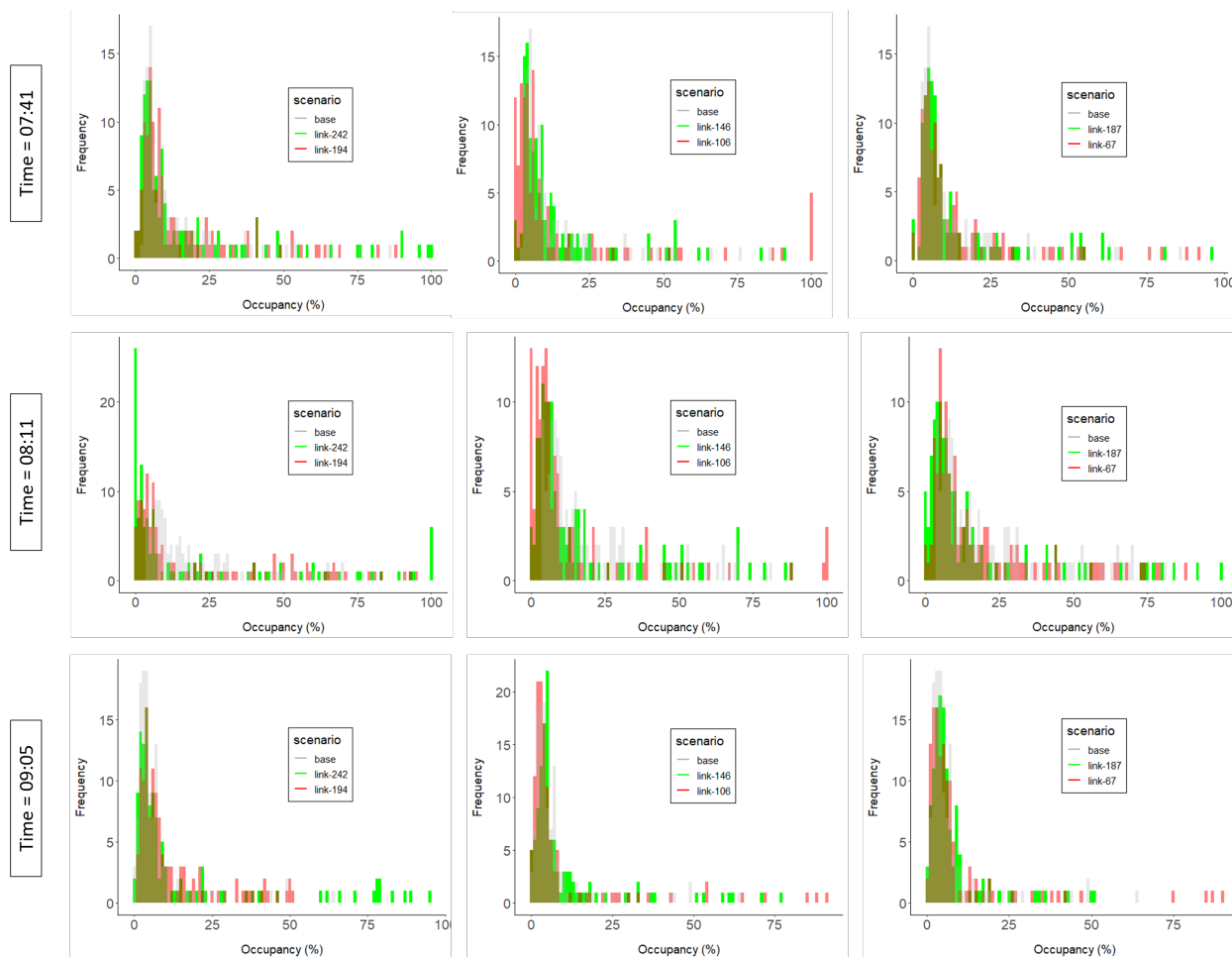


FIGURE 5 : Occupancy distribution across the links of the network during different time intervals for the selected scenarios.

1 index for links of a network by removing a link from the network and calculating the reduction in
 2 weighted average flow. Additionally, we observe that the closure of links with similar CS results
 3 in comparable changes in the shape of the MFD. This is particularly interesting since it enables us
 4 to develop incident detection algorithms. We can cluster the links of a given network into a limited
 5 number of clusters based on their criticality and then detect possible road closures by observing
 6 the changes in the shape of MFD. Thus, we can detect an incident by traffic measurements at other
 7 locations in the network. Moreover, the proposed CS is a proxy for redundancy in the network
 8 which lets us conclude that the MFD in networks with higher redundancy is more stable as drivers
 9 have more route choices. Such property was suggested in (37) as well.

10 As mentioned earlier, we designed our network similar to the one from Parzani et al. (44)
 11 to reproduce comparable MFDs. In their paper, the authors divide the network based on a route
 12 overlapping factor in five clusters and derive an MFD for each. For the cluster that is mainly com-
 13 posed of links at the center of the network, the MFD shows a higher trip production with a smaller
 14 hysteresis loop, whereas the cluster composed of links at boundaries shows smaller production and
 15 lower critical density. This implies that these links contribute less to the average MFD of the entire
 16 network and therefore, their closure would have minor impacts on the MFD.

1 Another finding of the study is related to the type of hysteresis loops. Two types of hystere-
2 sis loops were introduced in (34) We observe a third type of hysteresis loop in which flow increases
3 as occupancy decreases. This can happen during situations where several links of the network are
4 fully congested (at jam density) and inflow is near zero while outflow increases. Imagine a case
5 where a link is saturated and congestion propagates to the origin links which blocks the inflow
6 demand. Consequently, demand remains constant and flow is driven only by supply starts to dissi-
7 pate. In our specific case, for the scenarios where links 242 and 203 are closed, at the beginning
8 of the simulation the inflow is much larger than the outflow. After the peak in demand is reached,
9 the links of the network are mostly saturated and we have mainly outflow resulting in a signifi-
10 cant reduction of the inflow/outflow ratio. Once several links reach free-flow state again, this ratio
11 is balanced and the hysteresis loop is closed. From there, the unloading phase of the network
12 continues on the same curve as the loading phase.

13 We want to highlight another interesting observation made in this study. The point at which
14 the MFD obtained from the incident scenario diverges from the base MFD was the same in all of
15 scenarios. Interestingly, in the MFD of the base scenario the hysteresis loop starts exactly at the
16 same point. This implies that our network gets unstable at flow 400 veh/h/ln and occupancy 8%.
17 This behavior does not change with removing one link from the network for the same demand.
18 Even though we cannot generalize this conclusion, but the existence of a point at which bifurcation
19 occurs as a property of the network is valuable for the development of traffic control measures.

20 CONCLUSION AND FUTURE WORK

21 In this paper, we present a framework to study the macroscopic traffic dynamics in urban networks
22 during incidents. More specifically, we use a microscopic traffic simulation to study the charac-
23 teristics of the MFD and the induced hysteresis loop due to a road closure. We introduce a link
24 criticality score (CS) which reflects the changes in network redundancy by removing a link from
25 the network. An important finding of the study is that redundancy is directly connected to the shape
26 and size of the hysteresis loop. A higher number of alternative paths alleviates the impacts of road
27 closure by assisting the drivers to find alternative routes which results in an even distribution of
28 congestion across the network. The results of the simulation show that higher CS value imposes
29 larger hysteresis loops in the MFD. Such a property can be used to develop incident detection al-
30 gorithms for urban networks. The main advantage of this approach is that MFD can be estimated
31 by a limited number of loop detectors which most cities have already in place. In other words, our
32 proposed framework can detect incidents occurring on links without sensors by observing traffic
33 on other links in the same network.

34 One of the main limitations of this study is that the results may strongly rely on the assump-
35 tions regarding the network structure, the OD pairs, and drivers' route choice during incidents.
36 Therefore, future works will focus on different network structures with various demand profiles.
37 Moreover, the behavior of drivers while facing a closed road must be further investigated. The in-
38 fluence of route choice on the shape of MFD suggests that if drivers have access to real-time travel
39 information they may avoid the congestion, which significantly affects the characteristics of the
40 MFD. This was investigated in a previous study by the authors (45) in which they show that imple-
41 menting rerouting strategies can improve network production and avoid gridlock. Additionally, we
42 assumed detectors are located in a way that bias in the data is minimized. In reality, however, such
43 an assumption is rare and hence the bias from measurement on the shape of the hysteresis loop
44 should be studied. Such bias can also arise from the selection of time-space window for data ag-

1 gregation and needs a careful analysis, which was not covered in this study. Finally, our proposed
2 CS is static and does not consider the traffic condition. This indicator can be further improved by
3 taking into account the traffic volume or travel time of the links.

4 **AUTHORS CONTRIBUTION**

5 The authors confirm contribution to the paper as follows: study conception and design: Sasan
6 Amini and Fritz Busch; Simulation analysis and interpretation of results: Sasan Amini and Gabriel
7 Tilg; draft manuscript preparation: Sasan Amini, Gabriel Tilg and Fritz Busch. All authors re-
8 viewed the results and approved the final version of the manuscript.

REFERENCES

1. Busch, F., Incident detection. In *Concise Encyclopedia of Traffic & Transportation Systems*, Elsevier, 1991, pp. 219–225.
2. Mahmassani, H., C. Haas, S. Zhou, and J. Peterman, Evaluation of incident detection methodologies. *Research Report No. FHWA/TX-00/1795-1*, 1999.
3. Persaud, B. N., F. L. Hall, and L. M. Hall, Congestion identification aspects of the McMaster incident detection algorithm. *Transportation Research Record*, , No. 1287, 1990.
4. Margreiter, M., Automatic incident detection based on bluetooth detection in northern Bavaria. *Transportation research procedia*, Vol. 15, 2016, pp. 525–536.
5. Busch, F. and M. Fellendorf, Automatic incident detection on motorways. *Traffic Engineering & Control*, Vol. 31, No. 4, 1990.
6. Bell, M. G. and B. Thancanamootoo, Automatic incident detection within urban traffic control systems. *Proceedings of the Roads and Traffic Conference*, Vol. 4, No. 2, 1988.
7. Sethi, V., N. Bhandari, F. S. Koppelman, and J. L. Schofer, Arterial incident detection using fixed detector and probe vehicle data. *Transportation Research Part C: Emerging Technologies*, Vol. 3, No. 2, 1995, pp. 99–112.
8. Yuan, F. and R. L. Cheu, Incident detection using support vector machines. *Transportation Research Part C: Emerging Technologies*, Vol. 11, No. 3-4, 2003, pp. 309–328.
9. Anbaroglu, B., B. Heydecker, and T. Cheng, Spatio-temporal clustering for non-recurrent traffic congestion detection on urban road networks. *Transportation Research Part C: Emerging Technologies*, Vol. 48, 2014, pp. 47–65.
10. Anbaroglu, B., T. Cheng, and B. Heydecker, Non-recurrent traffic congestion detection on heterogeneous urban road networks. *Transportmetrica A: Transport Science*, Vol. 11, No. 9, 2015, pp. 754–771.
11. Zhang, Z., Q. He, H. Tong, J. Gou, and X. Li, Spatial-temporal traffic flow pattern identification and anomaly detection with dictionary-based compression theory in a large-scale urban network. *Transportation Research Part C: Emerging Technologies*, Vol. 71, 2016, pp. 284–302.
12. Godfrey, J., The mechanism of a road network. *Traffic Engineering & Control*, Vol. 8, No. 8, 1969.
13. Ardekani, S. and R. Herman, Urban Network-Wide Traffic Variables and Their Relations. *Transportation Science*, Vol. 21, No. 1, 1987, pp. 1–16.
14. Herman, R. and I. Prigogine, A two-fluid approach to town traffic. *Science*, Vol. 204, No. 4389, 1979, pp. 148–151.
15. Mahmassani, H., J. C. Williams, and R. Herman, Performance of urban traffic networks. In *Proceedings of the 10th International Symposium on Transportation and Traffic Theory*, 1987, pp. 1–20.
16. Daganzo, C. F. and N. Geroliminis, An analytical approximation for the macroscopic fundamental diagram of urban traffic. *Transportation Research Part B: Methodological*, , No. 42, 2008, pp. 771–781.
17. Geroliminis, N. and C. F. Daganzo, Existence of urban-scale macroscopic fundamental diagrams: Some experimental findings. *Transportation Research Part B: Methodological*, Vol. 42, No. 9, 2008, pp. 759–770.
18. Buisson, C. and C. Ladier, Exploring the impact of homogeneity of traffic measurements on the existence of macroscopic fundamental diagrams. *Transportation Research Record: Journal of*

- the Transportation Research Board*, Vol. 2124, 2009, pp. 127–136.
19. Tsubota, T., A. Bhaskar, and E. Chung, Macroscopic fundamental diagram for Brisbane, Australia. *Transportation Research Record: Journal of the Transportation Research Board*, Vol. 2421, 2014, pp. 12–21.
 20. Ambühl, L., A. Loder, M. Menendez, and K. W. Axhausen, Empirical macroscopic fundamental diagrams: New insights from loop detector and floating car data. *Transportation Research Record*, 2016.
 21. Ambühl, L., A. Loder, H. Becker, M. Menendez, and K. W. Axhausen, Evaluating London's congestion charge: An approach using the macroscopic fundamental diagram. In *7th Transport Research Arena (TRA 2018)*, IVT, ETH Zurich, 2018.
 22. Ji, Y., W. Daamen, S. Hoogendoorn, S. Hoogendoorn-Lanser, and X. Qian, Investigating the Shape of the Macroscopic Fundamental Diagram Using Simulation Data. *Transportation Research Record: Journal of the Transportation Research Board*, Vol. 2161, No. 1, 2010, pp. 40–48.
 23. Knoop, V. L., D. De Jong, and S. P. Hoogendoorn, Influence of road layout on network fundamental diagram. *Transportation Research Record*, Vol. 2421, No. 1, 2014, pp. 22–30.
 24. Duruisseau, C. and L. Leclercq, A Global Sensitivity Analysis of Dynamic Loading and Route Selection Parameters on Network Performances. *Journal of Advanced Transportation*, Vol. 2018, 2018.
 25. Knoop, V., S. Hoogendoorn, and J. Van Lint, Routing Strategies Based on Macroscopic Fundamental Diagram. *Transportation Research Record: Journal of the Transportation Research Board*, Vol. 2315, No. 2315, 2013, pp. 1–10.
 26. Yildirimoglu, M., M. Ramezani, and N. Geroliminis, Equilibrium analysis and route guidance in large-scale networks with MFD dynamics. *Transportation Research Procedia*, Vol. 9, 2015, pp. 185–204.
 27. Yildirimoglu, M., I. I. Sirmatel, and N. Geroliminis, Hierarchical control of heterogeneous large-scale urban road networks via path assignment and regional route guidance. *Transportation Research Part B: Methodological*, Vol. 118, 2018, pp. 106–123.
 28. Haddad, J., Robust constrained control of uncertain macroscopic fundamental diagram networks. *Transportation Research Procedia*, Vol. 7, 2015, pp. 669–688.
 29. Keyvan-Ekbatani, M., A. Kouvelas, I. Papamichail, and M. Papageorgiou, Exploiting the fundamental diagram of urban networks for feedback-based gating. *Transportation Research Part B: Methodological*, Vol. 46, No. 10, 2012, pp. 1393–1403.
 30. Cao, J. and M. Menendez, System dynamics of urban traffic based on its parking-related-states. *Transportation Research Part B: Methodological*, Vol. 81, 2015, pp. 718–736.
 31. Leclercq, L., A. Sénécat, and G. Mariotte, Dynamic macroscopic simulation of on-street parking search: A trip-based approach. *Transportation Research Part B: Methodological*, Vol. 101, 2017, pp. 268–282.
 32. Gayah, V. and C. F. Daganzo, Clockwise hysteresis loops in the Macroscopic Fundamental Diagram: An effect of network instability. *Transportation Research Part B: Methodological*, Vol. 45, No. 4, 2011, pp. 643–655.
 33. Saberi, M., H. S. Mahmassani, and A. Zockaie, Network capacity, traffic instability, and adaptive driving: findings from simulated urban network experiments. *EURO Journal on Transportation and Logistics*, Vol. 3, No. 3-4, 2014, pp. 289–308.
 34. Saberi, M. and H. S. Mahmassani, Hysteresis and Capacity Drop Phenomena in Freeway Net-

- works Empirical Characterization and Interpretation. *Transportation Research Record: Journal of the Transportation Research Board*, Vol. 2391, 2013, pp. 44–55.
35. Geroliminis, N. and J. Sun, Properties of a well-defined macroscopic fundamental diagram for urban traffic. *Transportation Research Part B: Methodological*, Vol. 45, No. 3, 2011, pp. 605–617.
 36. Shim, J., J. Yeo, S. Lee, S. H. Hamdar, and K. Jang, Empirical evaluation of influential factors on bifurcation in macroscopic fundamental diagrams. *Transportation Research Part C: Emerging Technologies*, Vol. 102, 2019, pp. 509–520.
 37. Geroliminis, N. and J. Sun, Hysteresis phenomena of a Macroscopic Fundamental Diagram in freeway networks. *Transportation Research Part A: Policy and Practice*, Vol. 45, No. 9, 2011, pp. 966–979.
 38. Zockaie, A., H. S. Mahmassani, M. Saberi, and Ö. Verbas, Dynamics of Urban Network Traffic flow during a Large-Scale Evacuation. *Transportation Research Record: Journal of the Transportation Research Board*, Vol. 2422, No. 1, 2014, pp. 21–33.
 39. Kim, S. and H. Yeo, Evaluating Link Criticality of Road Network based on the Concept of Macroscopic Fundamental Diagram Diagram. *Transportmetrica A: Transport Science*, Vol. 13, No. 2, 2016, pp. 162–193.
 40. Horiguchi, R., M. Iijima, M. Kobayashi, and H. Hanabusa, Traffic Anomaly Detection for Surface Street Networks With the Mesh-Wised Traffic Indices on Macroscopic Fundamental Diagram. *OPTIMUM 2013 – International Symposium on Recent Advances in Transport Modelling*, 2013, pp. 1–7.
 41. White, D. R. and S. P. Borgatti, Betweenness centrality measures for directed graphs. *Social networks*, Vol. 16, No. 4, 1994, pp. 335–346.
 42. Lopez, P. A., M. Behrisch, L. Bieker-Walz, J. Erdmann, Y.-P. Flötteröd, R. Hilbrich, L. Lücken, J. Rummel, P. Wagner, and E. Wießner, Microscopic Traffic Simulation using SUMO. In *The 21st IEEE International Conference on Intelligent Transportation Systems*, IEEE, 2018.
 43. Leclercq, L., N. Chiabaut, and B. Trinquier, Macroscopic Fundamental Diagrams: A cross-comparison of estimation methods. *Transportation Research Part B: Methodological*, Vol. 62, 2014, pp. 1–12.
 44. Parzani, C., L. Leclercq, N. Benoumechiara, and D. Villegas, Clustering route choices methodology for network performance analysis. *Transportmetrica B: Transport Dynamics*, Vol. 5, No. 2, 2017, pp. 191–210.
 45. Amini, S., G. Tilg, and F. Busch, Evaluating the impact of real-time traffic control measures on the resilience of urban road networks. In *2018 21st International Conference on Intelligent Transportation Systems (ITSC)*, IEEE, 2018, pp. 519–524.